

Copyright is owned by the Author of the thesis. Permission is given for a copy to be downloaded by an individual for the purpose of research and private study only. The thesis may not be reproduced elsewhere without the permission of the Author.

MOLECULAR DIFFUSION AS MEASURED BY PULSED  
FIELD GRADIENT NUCLEAR MAGNETIC RESONANCE

A thesis presented in partial fulfilment  
of the requirements for the degree  
of Master of Science  
in Chemistry at  
Massey University

JEREMY SAMUEL DRUCE KISSOCK

1982

## ABSTRACT

The work presented in this thesis may be conveniently divided into three sections.

Firstly the development of a Carr-Purcell-Meiboom-Gill pulse sequence for use in the pulsed field gradient experiment in order to examine diffusion over long diffusion times is described.

Secondly diffusion coefficients of both components of binary mixtures of methanol and benzene have been measured using pulsed field gradient fourier transform NMR. Results showed self-association to be dominant over AB association and a brief qualitative explanation of the reasons for this is given.

In the third section, which is the major part of this thesis, diffusion coefficients of water in the caesium perfluoro-octanoate, water system have been determined at various weight fractions and temperatures by pulsed field gradient NMR. The liquid crystalline phases occurring within the system are the isotropic micellar solution, the nematic amphiphilic mesophase and the smectic lamellar mesophase. Water was found to pass through the system in an unrestricted and virtually unhindered manner. These results were discussed in terms of the known structures of the phases and with respect to possible permeation mechanisms. No definite conclusion as to the permeation mechanism is possible. The limitations in the use of surfactants as membrane models is discussed.

ACKNOWLEDGEMENTS

I wish to thank my supervisor Dr. Kenneth Jolley for his constant encouragement and invaluable assistance and advice.

I am grateful also to Dr Paul Callaghan for his advice and assistance in the use of the NMR spectrometer, as well as to members of the chemistry department for their helpful comments and encouragement.

I thank the staff of the electronics workshop for their assistance and cooperation.

I am also most grateful to Janet Sayers and Lorraine Stewart for typing this thesis.

## TABLE OF CONTENTS

	page
Abstract	ii
Acknowledgements	iii
Abbreviations	vi
 <u>SECTION ONE</u>	
<u>NUCLEAR MAGNETIC RESONANCE THEORY</u>	
A. <u>Quantum Mechanical Treatment</u>	
1.1 NMR energy levels	1
1.2 The chemical shift	3
B. <u>Classical Treatment</u>	
1.3 Precession	3
1.4 The rotating frame of reference	4
1.5 The Bloch equations	7
1.6 Pulsed nuclear magnetic resonance	10
1.7 Measurement of relaxation times	14
1.8 Fourier analysis and Fourier transformation	16
1.9 Definition of the diffusion coefficient	18
1.10 Methods of Measurement of diffusion rates	19
1.11 Restricted diffusion	21
1.12 Inherent errors and their solution through a modified CPMG sequence	22
 <u>SECTION TWO</u>	
<u>EXPERIMENTAL PROCEDURES, METHODS AND EQUIPMENT</u>	
2.1 FX 60 description	24
2.2 Diffusion measurements	24
2.3 Temperature control and sample space geometry	25
2.4 Deuterium NMR spectra	26
2.5 Inherent errors in the use of a modified Hahn spin-echo sequence for diffusion experiments and the solution of this error by the use of a CPMG sequence	26

### SECTION THREE

3.1	Introduction	35
3.2	Experimental	35
3.3	Characterization of the D <sub>2</sub> O/CsPFO system	36
3.4	Results and discussion	43
	conclusion	67

### APPENDICES

A.1	<u>Diffusion rates of binary mixtures. A comparison between Fourier transform and isotopic methods</u>	
A.1.1.	Introduction	68
A.1.2	Experimental	68
A.1.3.	Results and discussion	69
A.2.	Integrated circuit information	73
	Bibliography	75

## ABBREVIATIONS

$A_{\infty}, A_{\tau}$	amplitudes of FID signal after $90^{\circ}$ pulse at times $t = \infty$ and $t = \tau$ in a $180^{\circ}, \tau, 90^{\circ}$ experiment
B	magnetic field
$B_0$	magnetic field (externally applied)
$B_1$	magnetic field from the radiofrequency pulse
$B_{\text{eff.}}$	an effective magnetic field, defined by equation 17
CsPFO	caesium perfluoro-octanoate
CPMG	Carr-Purcell-Meiboom-Gill
dc	direct current
D	diffusion coefficient
$D_{\perp}, D_{\parallel}$	components of D parallel and perpendicular to symmetry axis
$E_A$	activation energy
F I D	free induction decay
FT	Fourier transform
$g_0$	uniform and stationary field gradient
$g(\omega)$	absorption line shape, defined by equation [24]
G	magnetic field gradient
h	Planck's constant
$\hbar$	modfield Planck's constant, equal to $h/2\pi$
$\hat{i}$	unit vector along the x axis
I	nuclear spin quantum number
IC	integrated circuit
$\hat{j}$	unit vector along the y axis
k	Boltzmann constant
$\hat{k}$	unit vector along the z axis
LiPFO	lithium perfluoro-octanoate
$m_I$	direction of vector components of nuclear spin angular moments
M	macroscopic magnetization vector
$N_{\alpha}, N_{\beta}$	number of spins in the $\alpha$ and $\beta$ energy states, defined by equation 6
NMR	nuclear magnetic resonance
O.D.	outer diameter
$\underline{P}$	nuclear angular momentum vector
PFG	pulsed field gradient

PFO	perfluoro-octanoate
r.f.	radiofrequency
R	gas constant
RMS	root mean square
t	time
$t_1$	delay time in applying the first field gradient pulse
$t_2$	equal to $2\tau - (t_1 + \Delta + \delta)$
T	Kelvin temperature
$T_1$	longitudinal or spin-lattice relaxation time
$T_2$	transverse or spin-spin relaxation time
U	energy
$\Delta U$	separation between two energy levels
x,y,z	cartesian coordinate system axis
$\gamma$	magnetogyric ratio
$\delta$	duration of field gradient pulses
$\Delta$	separation between two field gradient pulses
$\theta$	angle
$\mu$	nuclear magnetic moment
$\nu_0, \omega_0$	resonance frequencies
$\sigma$	screening constant
$\omega$	angular frequency
$\tau$	time between pulses in a pulse sequence



1

SECTION ONE

NUCLEAR MAGNETIC RESONANCE THEORY

A. Quantum Mechanical Treatment (1,2)

1.1 N.M.R. Energy Levels

Most nuclei behave as though they possess spin angular momentum ( $\underline{P}$ ). The magnitude of  $\underline{P}$  is given by :

$$P = \hbar \sqrt{I(I+1)}$$

and its direction by  $m_I$  which are the components of  $\underline{P}$  along a reference direction.  $I$  is the quantum number for nuclear spin which can have half integral values and

$$m_I = +I, +I-1, \dots, -I.$$

e.g.  $^1\text{H} \dots I = 1/2$

(diagram 1)

magnitude of  $P = \hbar \sqrt{I(I+1)} = \sqrt{3/4} \hbar$

and  $m_I = +1/2$  or  $-1/2$

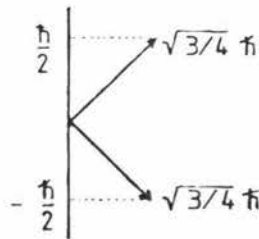


diagram 1

The spin and charge of the nucleus confers a magnetic moment ( $\mu$ ):

$$\begin{aligned} \underline{\mu} &= \gamma \hbar \underline{I} \\ \text{or } \mu_z &= \gamma \hbar m_I \\ &= \gamma P_z \end{aligned}$$

where  $\gamma$  is the magnetogyric ratio, the ratio of magnetic moment to angular momentum, and is a constant for a given nucleus.

The following discussion will be mainly confined to the  $I = 1/2$  nucleus since this thesis was primarily concerned with  $^1\text{H}$ .

If a steady magnetic field ( $B$ ) is applied to the nucleus there is an interaction between the field and the magnetic moment which may be represented by :

$$U = -\underline{\mu} \cdot \underline{B}$$

(where  $U$  is the energy of the interaction ). If the direction of the magnetic field is in the  $z$  direction the interaction may be rewritten :

$$U = -\mu_z \cdot B = -\gamma \hbar m_I B \quad [4]$$

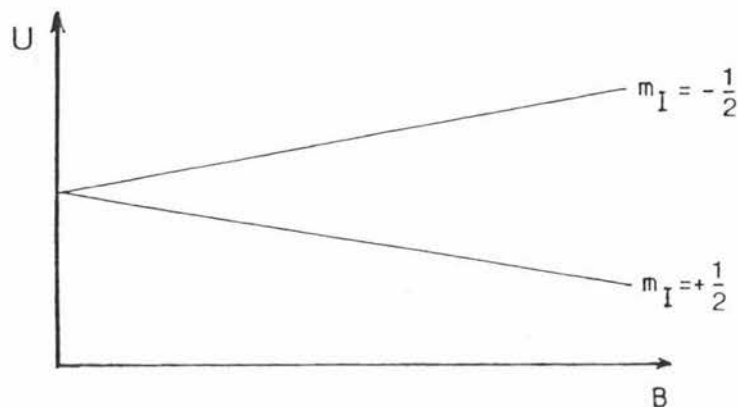


diagram 2

The selection rule for the transition between energy levels is  $\Delta m = \pm 1$ .

$$\Delta U = h\nu = \gamma \hbar B$$

$$\text{Therefore } \nu = \gamma B / 2\pi \quad [5]$$

where  $\nu$  is the frequency of radiation needed to bring about transition. Note that the energy separation depends upon the strength of the magnetic field (diagram 2 ).

The allowed values that the spins will take will be in a Boltzmann

distribution. If there are  $N_\alpha$  spins in the lower state and  $N_\beta$  spins in the upper state; the ratio of  $\alpha$  to  $\beta$  spins is:

$$\frac{N_\beta}{N_\alpha} = \exp(-\gamma \hbar B/kT) \quad [6]$$

For example:  $B_0 = 1.4$  Tesla  $T = 300$  K  
for a  $^1\text{H}$  nucleus.

$$\frac{N_\beta}{N_\alpha} = 0.9999905$$

That is, only a very small (but detectable) excess of spins exist in the lower,  $\alpha$ , state.

### 1.2 The Chemical Shift

The resonance lines from liquids are exceedingly narrow and consequently very small interactions can be detected. The two types of interaction which are important are the nuclear zeeman interaction and nuclear spin-spin coupling. The surrounding electrons in a molecule produce shielding effects which change the zeeman term from

$$U = -\gamma \hbar m_I B$$

to

$$U = -\gamma \hbar m_I (1 - \sigma) B \quad [7]$$

This is because the actual field at the nucleus is the sum of two magnetic fields;  $B$ , the applied field and  $-\sigma B$ , the local field at the nucleus arising from the induced electronic currents.

## B. Classical Treatment (1,2,3)

### 1.3 Precession

It can be shown by classical mechanics that the torque exerted on a magnetic moment by a magnetic field inclined at an angle  $\theta$  relative to the moment causes the magnetic moment to precess about the direction of the field (diagram 3).

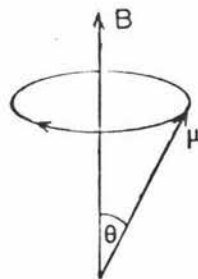


diagram 3

The frequency of precession is known as the Larmour frequency.

$$\frac{d\underline{P}}{dt} = \underline{\mu} \times \underline{B}$$

since  $\underline{\mu} = \gamma \underline{P}$

$$\frac{d\underline{\mu}}{dt} = \underline{\mu} \times (\gamma \underline{B}) \tag{8}$$

If  $\underline{B} = B_0 \hat{k}$ , where  $\hat{k}$  is the z unit vector, then the spin will precess at an angular frequency where

$$\omega_0 = -\gamma B_0 \tag{9}$$

1.4 The Rotating Frame of Reference

In the treatment of pulse methods it is usually simpler to refer the motion of magnetism to a coordinate system that rotates about  $B_0$  in the same direction which the nuclear moments precess, rather than the fixed coordinate system of the laboratory ( diagram 4 ).

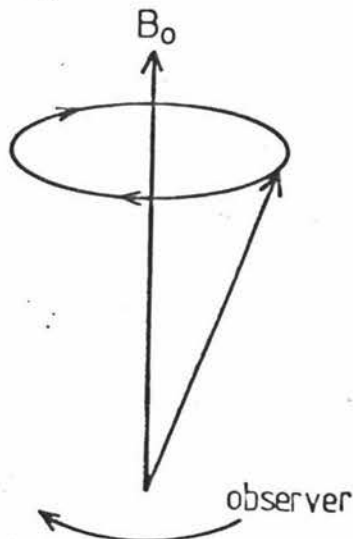
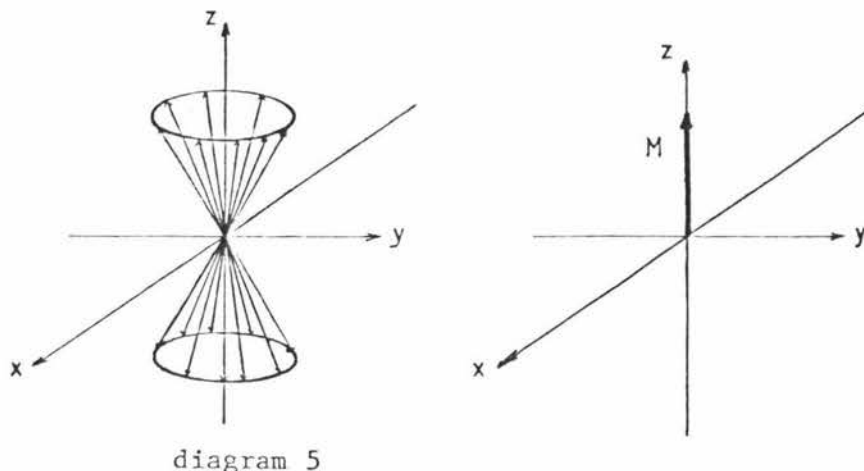


diagram 4

If  $\underline{M}$  is the vector sum of all the  $\underline{\mu}$ 's (diagram 5), then by summing equation 8 over all  $\underline{\mu}$  the following relation is obtained:

$$\frac{d\underline{M}}{dt} = \gamma \underline{M} \times \underline{B} \quad [10]$$



$\underline{M}$  can be considered in terms of components along the three cartesian axes:

$$\underline{M} = M_x \hat{i} + M_y \hat{j} + M_z \hat{k} \quad [11]$$

Therefore

$$\frac{d\underline{M}}{dt} = \left( \frac{\partial M_x}{\partial t} \hat{i} + \frac{\partial M_y}{\partial t} \hat{j} + \frac{\partial M_z}{\partial t} \hat{k} \right) + \left( \frac{M_x \partial \hat{i}}{\partial t} + \frac{M_y \partial \hat{j}}{\partial t} + \frac{M_z \partial \hat{k}}{\partial t} \right) \quad [12]$$

$\hat{i}$ ,  $\hat{j}$ ,  $\hat{k}$  are unit vectors and therefore their time derivatives can only rotate the vectors:

$$\frac{\partial \hat{i}}{\partial t} = \omega \times \hat{i}, \quad \frac{\partial \hat{j}}{\partial t} = \omega \times \hat{j}, \quad \frac{\partial \hat{k}}{\partial t} = \omega \times \hat{k} \quad [13]$$

The speed and direction of the unit vectors are defined by the same  $\omega$ ; hence equation [12] becomes:

$$\left( \frac{d\underline{M}}{dt} \right)_{\text{fixed}} = \frac{\partial \underline{M}}{\partial t} + \omega \times (M_x \hat{i} + M_y \hat{j} + M_z \hat{k})$$

$$= \left( \frac{\partial \underline{M}}{\partial t} \right)_{\text{rot}} + \underline{\omega} \times \underline{M} \quad [14]$$

From equation [10]

$$\left( \frac{d\underline{M}}{dt} \right)_{\text{fixed}} = \gamma \underline{M} \times \underline{B}$$

and from equation [14]

$$\left( \frac{d\underline{M}}{dt} \right)_{\text{rot}} = \gamma \underline{M} \times \underline{B} - \underline{\omega} \times \underline{M}$$

rearranging:

$$\begin{aligned} \left( \frac{d\underline{M}}{dt} \right)_{\text{rot}} &= \gamma \underline{M} \times \underline{B} + \gamma \underline{M} \times \frac{\underline{\omega}}{\gamma} \\ &= \gamma \underline{M} \times \left( \underline{B} + \frac{\underline{\omega}}{\gamma} \right) \end{aligned} \quad [15]$$

The term  $\underline{\omega} / \gamma$  can be considered as a fictitious field that arises from the effect of the rotation. Alternatively equation [15] may be rewritten :

$$\left( \frac{d\underline{M}}{dt} \right)_{\text{rot}} = \gamma \underline{M} \times \underline{B}_{\text{eff}}, \quad [16]$$

where  $\underline{B}_{\text{eff}}$  is the effective field, that is :

$$\underline{B}_{\text{eff}} = \underline{B} + \underline{\omega} / \gamma \quad [17]$$

In the rotating frame, therefore,  $\underline{M}$  precesses about  $\underline{B}_{\text{eff}}$ . If in addition to  $\underline{B}$  a radiofrequency field  $B_1$  is applied at right angles, then in the rotating frame at the Larmor frequency

$$\underline{B}_{\text{eff}} = B_0 + \underline{\omega}_0 / \gamma + B_1$$

and the fictitious field exactly cancels  $B_0$  along the  $z$  axis and leaves only  $B_1$  in the  $xy$  plane to interact with  $M$ . However in most situations  $B_1$  and the rotating frame move at a frequency different from the resonance frequency as so the relation depicted in diagram 6 occurs where the fictitious field does not cancel  $B_0$  and leaves a component of the effective field in the  $z'$  direction.

Mathematically the result is:

$$|B_{\text{eff}}| = [(B_0 - \omega/\gamma)^2 + B_1^2]^{1/2}$$

$$= (1/\gamma) [(\omega_0 - \omega)^2 + (\gamma B_1)^2]^{1/2}$$

Providing  $B_1 \gg (\omega_0 - \omega)$  then  $B_{\text{eff}} = B_1$

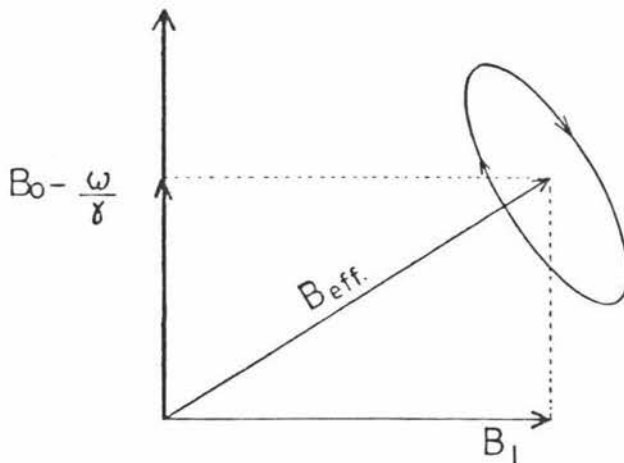


diagram 6

### 1.5 The Bloch Equations

Bloch et al. (4) found that the motion of the macroscopic magnetization in the presence of a magnetic field could be explained in terms of differential equations.

The vector product of equation [10] may be expanded in terms of components along the three cartesian axes and the unit vectors along these axes.

$$\begin{aligned}
 \underline{M} \times \underline{B} &= ( \hat{i} M_x + \hat{j} M_y + \hat{k} M_z ) \times ( \hat{i} B_x + \hat{j} B_y + \hat{k} B_z ) \\
 &= \hat{k} M_x B_y - \hat{j} M_x B_z - \hat{k} M_y B_x + \hat{i} M_y B_z \\
 &\quad + \hat{j} M_z B_x - \hat{i} M_z B_y \\
 \Leftrightarrow \underline{M} \times \underline{B} &= ( M_y B_z - M_z B_y ) \hat{i} + ( M_z B_x - M_x B_z ) \hat{j} \\
 &\quad + ( M_x B_y - M_y B_x ) \hat{k} \qquad [18]
 \end{aligned}$$

In general this equation consists of both the static applied field,  $B_0$ , and the magnetic vector of the r.f. field,  $B_1$ . The radio frequency field can be thought of as two vector fields rotating in opposite directions ( diagram 7 ).

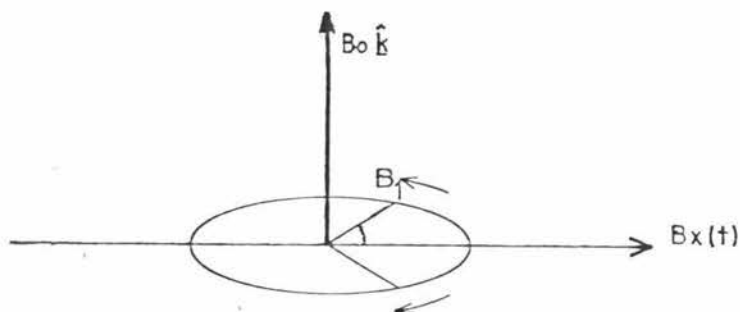


diagram 7

$$\begin{aligned}
 \underline{B} (t) &= B_x(t) \hat{i} = 2B_1 \cos \omega t \hat{i} \\
 &= B_1 [ \hat{i} \cos \omega t + \hat{j} \sin \omega t ] + B_1 [ \hat{i} \cos \omega t - \hat{j} \sin \omega t ] \\
 &\qquad \qquad \qquad [19]
 \end{aligned}$$

The only field that needs to be considered is the one that rotates in the same direction as the nuclear moments, therefore

$$B_1(t) = B_1 [ \hat{i} \cos \omega t - \hat{j} \sin \omega t ] \qquad [20]$$



Hence 
$$\frac{dM_x}{dt} = \gamma B_0 M_y + \gamma M_z B_1 \sin \omega t \quad [20]a$$

$$\frac{dM_y}{dt} = -\gamma B_0 M_x + \gamma M_z B_1 \cos \omega t \quad [20]b$$

$$\frac{dM_z}{dt} = 0 - \gamma M_x B_1 \sin \omega t - \gamma M_y B_1 \cos \omega t \quad [20]c$$

These equations are not complete since they do not account for the relaxation that must occur following a r.f. pulse. Decay to equilibrium occurs via a first order process with  $M_x$  and  $M_y$  decaying to zero and  $M_z$  to the equilibrium value of  $M_0$ . Hence:

$$\frac{dM_z}{dt} = -\gamma M_x B_1 \sin \omega t - \gamma M_y B_1 \cos \omega t + \frac{M_0 - M_z}{T_1} \quad [21]$$

$$\frac{dM_x}{dt} = \gamma B_0 M_y + \gamma M_z B_1 \sin \omega t - \frac{M_x}{T_2} \quad [22]$$

$$\frac{dM_y}{dt} = -\gamma B_0 M_x + \gamma M_z B_1 \cos \omega t - \frac{M_y}{T_2} \quad [23]$$

These are the Bloch equations.  $T_1$  and  $T_2$  are the longitudinal and transverse relaxation times respectively since they are time constants for decay along and perpendicular to  $B_0$ .

There are two methods for observing nuclear magnetic resonance; the continuous wave technique and pulse methods. The continuous wave method consists of sweeping the frequency of the r.f. field applied to a sample in a fixed magnetic field (or sweeping  $B_0$  with a fixed r.f. field). The signal is observed as an absorption line. The pulse method makes use of short bursts of r.f. power at a discrete frequency with the observation of the nuclear spin system being made after the r.f. field is turned off. Pulse methods are the superior being quicker and more versatile.

In the continuous wave experiment  $B_1$  is small and the sweep rate is slow.

$$\text{i.e. } \frac{dM}{dt} \text{ } x,y,z = 0$$

Under these conditions the Bloch equations can be solved to give the line shape for the absorption signal  $g(\omega)$ . The line shape is Lorentzian and is given by (2) :

$$g(\omega) = \frac{K T_2}{1 + T_2^2 (\omega_0 - \omega)^2} \quad [24]$$

K is a constant.

### 1.6 Pulsed Nuclear Magnetic Resonance

If the r.f. field, at the Larmor frequency, is turned on for a time  $t$ , then viewed in the rotating frame the effective field becomes aligned with the x axis and the magnetization vector will begin to tip towards this axis (diagram 8).

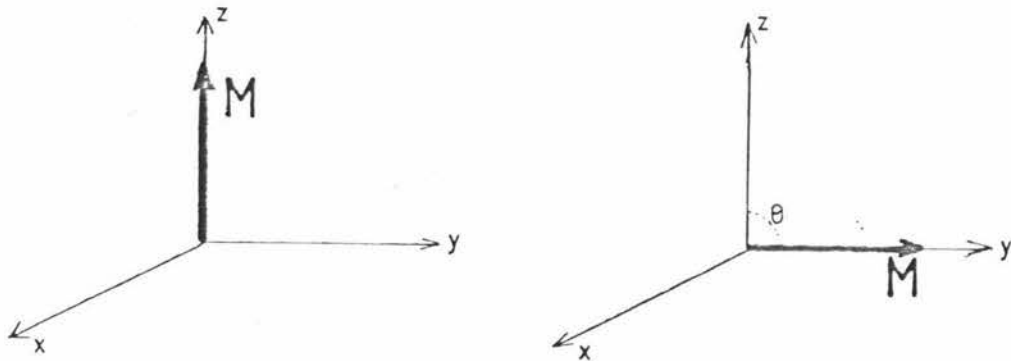


diagram 8

$$\theta = \omega_{\text{eff}} t = \gamma B_{\text{eff}} t = \gamma B_1 t$$

$$\text{i.e. } t = \frac{\theta}{\gamma B_1} \quad [25]$$

When  $B_1$  is off the magnetization will return to its equilibrium value along  $B_0$ .

Evolution of  $M_z$  following a  $180^\circ$  pulse

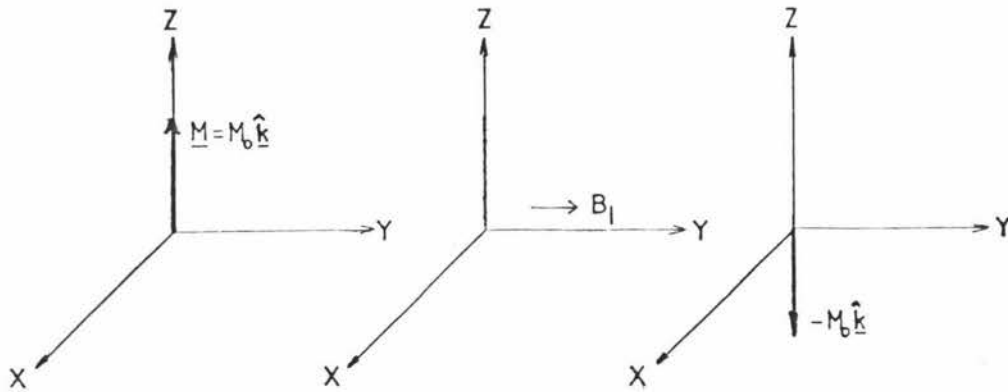


diagram 9

The evolution starts immediately following the  $90^\circ$  pulse.

$$M_z(t=0) = -M_0$$

$$M_x(0) = 0$$

$$M_y(0) = 0$$

using the Bloch equations :

$$\frac{dM_z}{dt} = \frac{M_0 - M_z}{T_1}$$

$$\int_{M=M_0}^{M_z} \frac{dM_z}{M - M_0} = \int_{t=0}^t \frac{dt}{T_1}$$

$$M_z(t) = M_0 \left( 1 - 2\exp\left(-\frac{t}{T_1}\right) \right) \quad (\text{diagram 10})$$

[26]

Evolution of  $M_x$ ,  $M_y$  and  $M_z$  following a  $90^\circ$  pulse ( diagram 12 ).

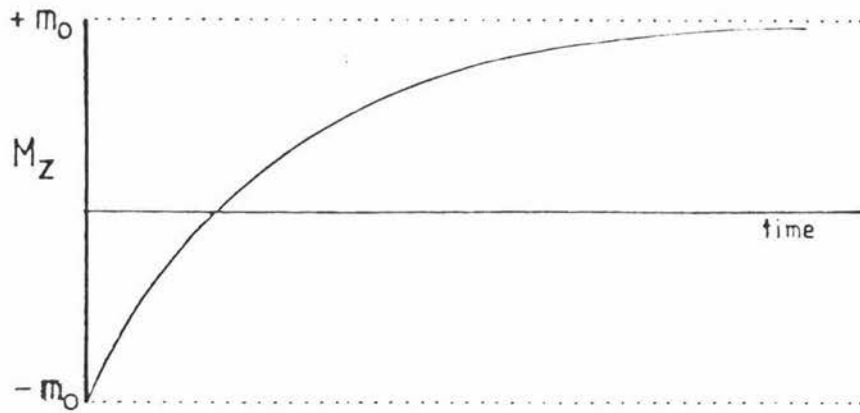


diagram 10

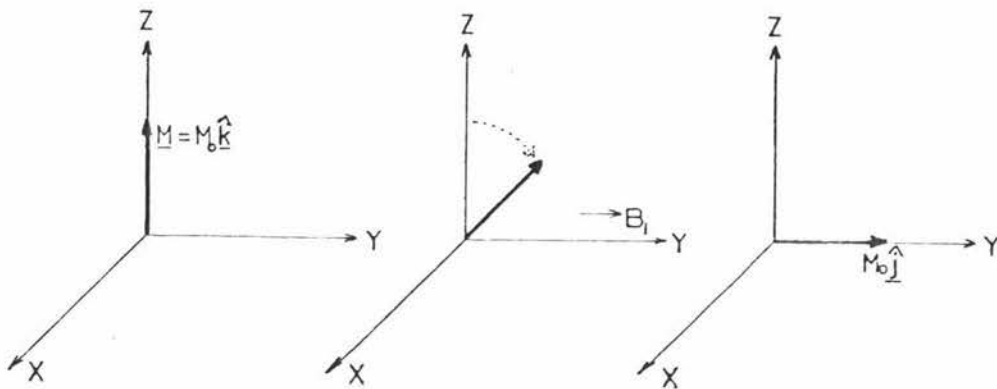


diagram 11

$$M_z(0) = 0, M_x(0) = 0, M_y(0) = 0$$

Using the Bloch equations :

(a) Evolution of  $M_z$

$$\int_{M=0}^{M_z} \frac{dM}{M_0 - M_z} = \int_{t=0}^t \frac{dt}{T_1}$$

$$\Rightarrow -\ln(M_0 - M_z) + \ln M_0 = t/T_1$$

$$\Leftrightarrow M_z(t) = M_0 (1 - \exp(-t/T_1))$$

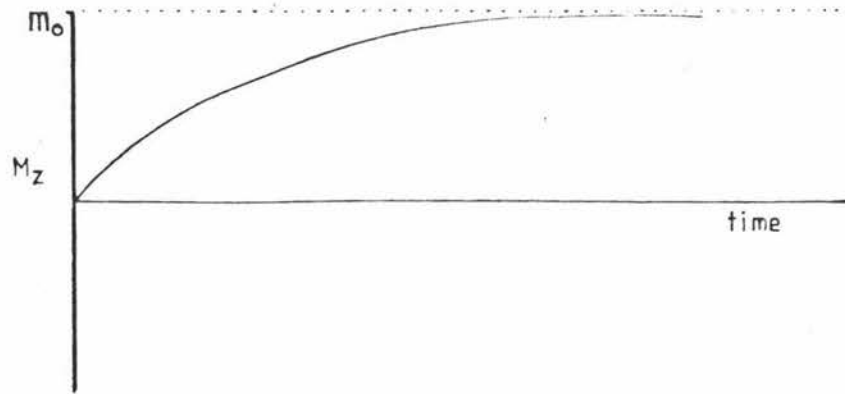


Diagram 12

(b) Evolution of  $M_x$

$$\frac{dM_x}{dt} = \gamma M_y B_0 - \frac{M_x}{T_2}$$

$$\frac{d^2 M_x}{dt^2} = \gamma B_0 \frac{dM_y}{dt} - \frac{dM_x}{dt} \frac{1}{T_2}$$

Substituting firstly for  $dM_y/dt$  from equation [20]b and secondly for  $M_y$  from equation [20]a gives a second order differential equation which has the solution:

$$\begin{aligned} M_x(t) &= M_0 \exp(-t/T_2) \sin \gamma B_0 t \\ &= M_0 \exp(-t/T_2) \sin 2 \pi \nu_0 t \end{aligned}$$

The resulting spectrum is known as a free induction decay or FID:

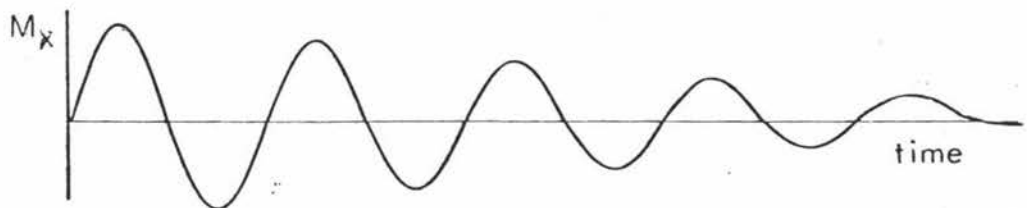


diagram 13

Similarly it can be shown that :

$$M_y(t) = M_0 \exp(-t/T_2) \cos 2\pi \nu_0 t \quad [28]$$

### 1.7 Measurement of Relaxation Times

#### (a) $T_1$ by Inversion Recovery

This is the most common procedure used. It consists of varying  $\tau$  in the  $180^\circ - \tau - 90^\circ$  pulse sequence. The  $180^\circ$  pulse takes  $\underline{M}$  out of thermal equilibrium, but still along the z axis. After a time  $\tau$  a  $90^\circ$  pulse takes the remaining  $M_z$  into the transverse plane so that its magnitude can be detected in the transverse detector coils. From equation [26] :

$$\ln (A_\infty - A_\tau) = \ln 2A_\infty - \tau/T_1 \quad [29]$$

$A_\tau$  is the initial amplitude of the F.I.D. following the  $90^\circ$  pulse at a time  $\tau$ , and  $A_\infty$  is the limiting value for a very long interval between the  $180^\circ$  and  $90^\circ$  pulses.  $T_1$  is determined from the slope of a plot of  $\ln (A_\infty - A_\tau)$  versus  $\tau$ .

#### (b) Measurement of $T_2$

If  $B_0$  was perfectly homogeneous then one could determine  $T_2$  simply by observing the decay of  $M_{x,y}$  after a  $90^\circ$  pulse. Because  $B_0$  is not perfectly homogeneous some of the nuclear magnets precess faster than  $\omega_0$  and some slower. Dephasing of spins therefore occurs, lowering  $M_{x,y}$  and shortening the observed  $T_2$ .

Because of this problem  $T_2$  is commonly measured by the modified Hahn spin-echo method (5). This method greatly reduces the effect of

field inhomogeneities. It consists of the application of a  $90^\circ/x - \tau - 180^\circ/y$  pulse sequence and the observation at a time  $2\tau$  of the free induction echo. The full Hahn expression is:

$$A(2\tau) \propto \exp\left[\frac{-2\tau}{T_2} - \frac{2}{3} \gamma^2 G^2 D \tau^3\right] \quad [30]$$

This equation shows that the echo amplitude does not decay in a simple exponential fashion. The spin-echo method is limited in its range of applicability due to the effect of molecular diffusion. If diffusion causes nuclei to move from one part of an inhomogeneous field to another the echo amplitude is reduced. The effect of diffusion is particularly pronounced for large values of  $\tau$  and thus may affect measurements of long  $T_2$ .

Carr-Purcell-Meiboom-Gill method for measuring  $T_2$  (CPMG) (6,7)

Because of the limited range in applicability of the spin-echo method a CPMG sequence may often be used. The pulse sequence used in this study consists of a  $90^\circ/x - \tau - 180^\circ/y - 2\tau - 180^\circ/-y - 2\tau - \dots$  sequence with observation of echo heights at  $2\tau, 4\tau, 6\tau, 8\tau, \dots$ . There are two distinct advantages of the CPMG sequence. Firstly; there is a considerable saving in time, for a train of  $n$  echoes may be obtained in a single sequence. Secondly; the effect of diffusion may be virtually eliminated by making  $\tau$  short since it is only during a time  $2\tau$  that diffusion is effective in reducing the amplitude of an echo. For the CPMG sequence:

$$A(t) \propto \exp\left[\frac{-t}{T_2} - \frac{1}{3} \gamma^2 G^2 D \tau^2 t\right] \quad [31]$$

Note the  $\tau^2$  term of the CPMG method compared with the  $\tau^3$  term of the spin-echo method. The change of phase of the  $180^\circ$  pulses from the initial  $90^\circ$  pulse (from being applied along the  $x$  axis, to the  $y$  axis) and the change in direction of application of the r.f. pulses ( $y, -y, y$  etc.) reduces the cumulative error from the not exactly accurate pulse time,  $t_p$ .

### 1.8 Fourier Analysis and Fourier Transformation

It is often useful to sort out what frequencies are present in a complex waveform and to determine the intensity of each of the frequencies present. By using the principles of fourier analysis it is possible to transform from the F.I.D. to the corresponding frequencies. A function  $A(t)$  can usually be expressed as an infinite series of sines and cosines :

$$A(t) = \sum_{n=0}^{\infty} A_n \cos(n\pi/T)t + \sum_{n=1}^{\infty} B_n \sin(n\pi/T)t \quad [32]$$

( $A_n$  and  $B_n$  are variable constants)

The r.f. signal emitted by the sample induces an oscillating e.m.f.,  $\delta(t)$ , in the probe detector coil :

$$\delta(t) = \delta_0 \exp(-t/T_2) \sin 2\nu_0 \pi t \quad [33]$$

A phase sensitive detector is used to shift the signal to the audio range :

$$\delta(t) = \delta_0 \exp(-t/T_2) \{ a \sin 2\pi \Delta \nu t + \beta \cos 2\pi \Delta \nu t \} \quad [34]$$

where  $\Delta \nu = \nu_0 - \nu_{ref}$  and  $a$  and  $\beta$  depend upon the phase setting of the r.f. reference.

$$a^2 + \beta^2 = 1 \quad [35]$$

(a) Sine Transform

$$\begin{aligned} F^S(\nu) &= \int_{t=0}^{\infty} \delta(t) \sin 2\pi \nu t \, dt \\ &= \delta_0 a \int_{t=0}^{\infty} \exp(-t/T_2) \sin 2\pi \Delta \nu t \sin 2\pi \nu t \, dt \\ &\quad + \delta_0 \beta \int_{t=0}^{\infty} \exp(-t/T_2) \cos 2\pi \Delta \nu t \sin 2\pi \nu t \, dt \\ &= \frac{\delta_0 a}{2} \left\{ \frac{(1/T_2)}{(1/T_2)^2 + (2\pi(\nu - \Delta \nu))^2} - \frac{(1/T_2)}{(1/T_2)^2 + (2\pi(\nu + \Delta \nu))^2} \right\} \end{aligned}$$



$$+ \frac{\delta_o \beta}{2} \left\{ \frac{2\pi(\nu + \Delta\nu)}{(1/T_2)^2 + (2\pi(\nu - \Delta\nu))^2} + \frac{2\pi(\nu - \Delta\nu)}{(1/T_2)^2 + (2\pi(\nu - \Delta\nu))^2} \right\}$$

[36]

(b) Cosine Transformation

$$\begin{aligned} F^C(\nu) &= \int_{t=0}^{\infty} \delta(t) \cos 2\pi\nu t \, dt \\ &= \frac{\delta_o a}{2} \left\{ \frac{2\pi(\nu + \Delta\nu)}{(1/T_2)^2 + (2\pi(\nu + \Delta\nu))^2} - \frac{2\pi(\nu - \Delta\nu)}{(1/T_2)^2 + (2\pi(\nu - \Delta\nu))^2} \right\} \\ &+ \frac{\delta_o \beta}{2} \left\{ \frac{(1/T_2)}{(1/T_2)^2 + (2\pi(\nu - \Delta\nu))^2} + \frac{1/T_2}{(1/T_2)^2 + (2\pi(\nu + \Delta\nu))^2} \right\} \end{aligned}$$

[37]

Only the positive frequencies are displayed. To obtain an absorption spectrum it may be necessary to admix the positive frequency parts of  $F^S(\nu)$  and  $F^C(\nu)$  in the proportions

$$aF^S(\nu) + \beta F^C(\nu)$$

The result is :

$$A = \frac{\delta_o}{2} (a^2 + \beta^2) \left\{ \frac{(1/T_2)}{(1/T_2)^2 + (2\pi(\nu - \Delta\nu))^2} \right\} \quad [38]$$

Where A is the absorption peak height. The shape of the curve is a Lorentzian curve :

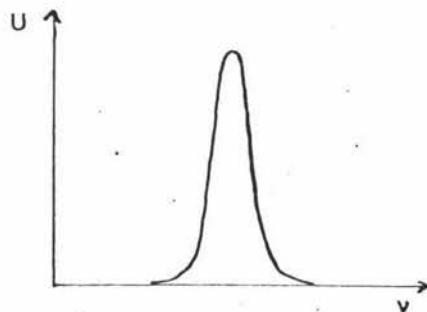


diagram 14

The frequency width at half the maximum peak height equals  $1/\pi T_2$ , therefore  $T_2$  is measurable from the absorption signal. This method will be disadvantageous if either :

(i) Broadening from magnetic field inhomogeneities occurs.

(ii) There is a broadening due to overlapping peaks of similar chemical shift.

### 1.9 Definition of the Diffusion Coefficient

Molecular migration in condensed phases may be treated as point to point jumps of the elementary particles governed by a rate constant (8).

Consider the simple case of a system with molecules which are sufficiently alike so that the whole may be thought of as forming a more or less perfect lattice.

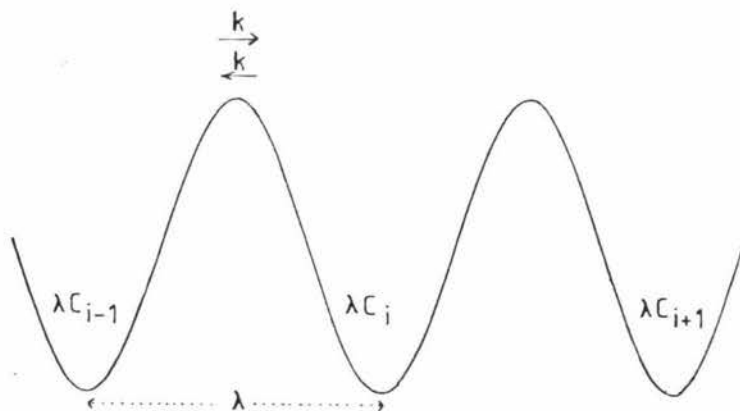


diagram 15

If  $C_i$  is the concentration per cubic centimeter at the  $i^{\text{th}}$  position, then the amount of material in a volume with a cross section of one square centimeter and length  $\lambda$  is  $\lambda C_i$  (diagram 15). Let  $K$  represent the number of times per second a molecule jumps, and  $Q$  be the amount of  $C$  passing per second through a square centimeter of surface, then :

$$Q = K \lambda C_i - K \lambda C_{i+1} \quad [39]$$

The concentration gradient between the  $i^{\text{th}}$  and the  $(i + 1)^{\text{th}}$  position is :

$$\frac{dc}{dx} = \frac{C_{i+1} - C_i}{\lambda} \quad [40]$$

Thus

$$Q = K\lambda(C_i + C_{i+1}) = \frac{-K\lambda^2(C_{i+1} - C_i)}{\lambda} \quad [41]$$

$$= -K\lambda^2 \frac{dC}{dx}$$

This is Fick's First Law , normally written as:

$$Q = -D \frac{dC}{dx} \quad [42]$$

where  $D = K\lambda^2$

i.e. D has dimensions  $L^2 T^{-1}$

### 1.10 Methods of Measurement of Diffusion Rates

#### (1) Steady Gradient Technique

The full modified Hahn spin-echo equation is:

$$A(2\tau) = K \exp[-2\tau/T_2 - 2/3 \gamma^2 G^2 D \tau^3] \quad [30]$$

where K is a constant. D can be measured by setting up an experiment to eliminate the first term of this sequence  $(-2\tau/T_2)$  , i.e. by keeping  $\tau$  constant and varying G. The result is :

$$\frac{A_G}{A_0} = \exp\left(-\frac{2}{3} \gamma^2 G^2 D \tau^3\right) \quad [43]$$

In principle D can be measured over a wide range but in practice there are limitations :

(a) It is extremely difficult to achieve  $\tau$  values of

less than 50  $\mu$  sec.

(b) The magnetic field gradient , G , must be present at all times, As G becomes larger ( in order to measure the slower diffusion rates ) the width of the echo envelope becomes smaller. The consequences of this are

(i) the information available from the echo decreases ,  
(ii) the band width of the detection system must be increased to observe the narrower echoes , lowering the signal / noise , and

(iii) with increasing linewidth the power output of the pulse transmitter will have to be increased to keep the r.f. field amplitude ,  $B_1$  , greater than the linewidth.

As a result of these problems the best results yet reported have a reproducibility of  $\pm 1\%$  and an overall accuracy of  $\pm 2\%$  (9). Furthermore , for systems in which the diffusion coefficient is spatially dependent it is desirable that the precise period of time during which diffusion is being observed be clearly defined. It is also desirable to make this time as short as possible.

(2) The Pulsed Field Gradient Method (10)

This consists of applying two magnetic field gradient pulses (G) of duration  $\delta$  before and after the  $180^\circ$  pulse of the modified Hahn spin-echo method ( diagram 16 )

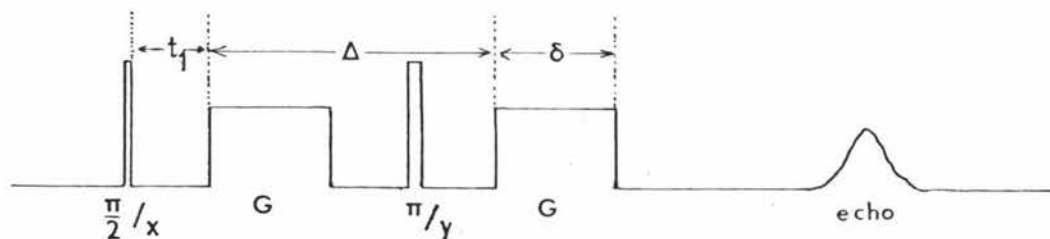


diagram 16

On application of the first gradient pulse there is a nearly instantaneous phase shift depending upon the location of each nucleus , a phase shift which records its position in the magnetic field.

This phase shift persists until it is inverted by the  $180^\circ$  pulse. A second phase shift occurs on application of the second gradient pulse. A nucleus which has had no net movement from its original position will refocus completely. Any motion that has occurred results in incomplete refocusing. This, therefore, is a method for detecting net motion during a time interval  $(\Delta - \delta/3)$ . The effect on the echo amplitude by the application of the two gradient pulses is given by (10):

$$\ln[A(2\tau)/A(0)] = -\gamma^2 D \left\{ \frac{2\tau^3}{3} g_0^2 + \delta^2 (\Delta - \delta/3) G^2 - \delta [(t_1^2 + t_2^2) + \delta(t_1 + t_2) + \frac{2\delta^2}{3} - 2\tau^2] G \cdot g_0 \right\} \quad [44]$$

where  $t_2 = 2\tau - (t_1 + \Delta + \delta)$  and is the time between the end of the second gradient pulse and the peak of the echo,  $t_1$  is the time at which the first gradient pulse occurs, and  $g_0$  is a uniform and stationary field gradient (due to field inhomogeneity). When  $G$  vanishes the result is the same as that obtained by the two pulse steady gradient spin-echo experiment, as expected. As  $g_0$  approaches zero (but not equal to zero since then there would be no loss of phase coherence) only the term in  $G^2$  remains and the result is:

$$\ln[A(2\tau)/A(0)] = -\gamma^2 D G^2 \delta^2 (\Delta - \delta/3) \quad [45]$$

When  $\tau$  ( $\Delta$ ),  $g_0$  or  $G$  are large then all three terms in the general equation may contribute. However if  $\tau$  (or  $\Delta$ ) and  $g_0$  are small the diffusion coefficient can be determined by varying either  $G$  or  $\Delta$ . Of the two variables,  $G$  is normally varied. In practice the direct determination of  $G$  is tedious and inaccurate. It is, therefore, usual to vary the current,  $I$ , supplied to the field gradient coils and to plot  $\ln A(G)/A(0)$  versus  $\gamma^2 \delta^2 (\Delta - \delta/3) I^2$  and determine the diffusion coefficient from the slope. This is possible for the use of water at  $25^\circ\text{C}$ , where  $D$  is known, a conversion factor between  $I$  and  $G$  can be calculated.

### 1.11 Restricted Diffusion

$(\Delta - \delta/3)$  may be regarded as the effective diffusion time for the

experiment. The experimental mean square distance is thus :  
 $\bar{z}^2 = 2D(\Delta - \delta/3)$  (11) . Since  $\Delta$  is the order of a few milliseconds restricted diffusion effects may become visible . In practice  $\bar{z}^2$  is required to be greater than  $(100 \text{ nm})^2$  for any significant attenuation to be observed. If within a system there are no barriers or obstructions to the diffusing species , or if there are barriers they are separated by distances greater than the distances being experimentally observed , then unrestricted diffusion will be observed. Such diffusion may be regarded as being in three dimensions. This , however , is not always the case for in some systems layers or capillaries may exist with dimensions smaller than the experimental mean square distance that is being measured. If such a system is in layers , diffusion will be observed as being in two dimensions. If the system exists as capillaries , diffusion will occur in only one dimension. From the linearity , or non-linearity , of the  $\ln[A(G)/A(0)]$  versus  $G^2$  plot information as to whether the system is unrestricted , layered or in capillaries and the distance between the barriers may be obtained (21).

### 1.12 Inherent Errors and Their Solution Through a Modified CPMG Sequence (12)

As stated previously ; when  $g_0$  and  $\tau$  ( or  $\Delta$  ) are of significant magnitude then all three terms in the general equation of the pulsed field gradient technique may contribute. This problem may be overcome by using a modified CPMG sequence. A  $\pi/2$  pulse is followed by a series of pairs of  $\pi_y$  and  $\pi_{-y}$  pulses , each  $\pi$  pulse following at a time  $2\tau$  after the previous one. Application of the first field gradient pulse is during an interval when the nuclei are dephasing. The second field gradient pulse is applied during a rephasing interval at a time  $\Delta$  after the first one (diagram 17 ).

The result is (12) :

$$\begin{aligned} \ln[A(t_n)/A(0)] = & - (t_n/T_2) \\ & + (-\gamma^2 D \left\{ 1/12 n^2 g_0^2 t_n^3 + G^2 \delta^2 (\Delta - \frac{1}{3} \delta) \right. \\ & \left. - G_0 \delta [(t_1^2 + t_3^2) + \delta(t_1 + t_3) + \frac{2\delta^2}{3} - 2\tau^2] \right\}) \end{aligned} \quad [46]$$

Where  $A(t_n)$  is the amplitude of the echo that forms at the time  $t_n$  and  $t_3 = \tau - t_1 - \delta$

Unless  $g_0$  is very large this can be approximated by:

$$\ln [A(t_n)/A(0)] = -\gamma^2 D G^2 \delta^2 (\Delta - \delta/3) \quad [47]$$

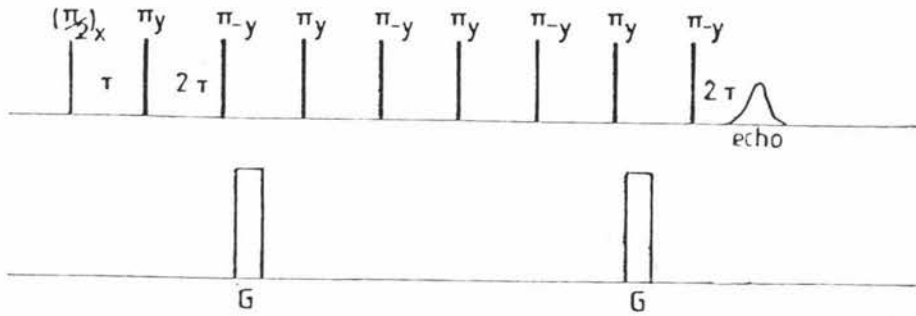


diagram 17

If only  $\Delta$  is varied the effect of field inhomogeneity is removed and equation [47] becomes an equality.